



HAL
open science

Comparison of ring currents evaluated consistently at Density Functional and Hartree-Fock levels

Remco Havenith, Anthony Meijer, Benjamin Irving, Patrick Fowler

► **To cite this version:**

Remco Havenith, Anthony Meijer, Benjamin Irving, Patrick Fowler. Comparison of ring currents evaluated consistently at Density Functional and Hartree-Fock levels. *Molecular Physics*, 2009, 107 (23-24), pp.2591-2600. 10.1080/00268970903449396 . hal-00548166

HAL Id: hal-00548166

<https://hal.science/hal-00548166>

Submitted on 19 Dec 2010

HAL is a multi-disciplinary open access archive for the deposit and dissemination of scientific research documents, whether they are published or not. The documents may come from teaching and research institutions in France or abroad, or from public or private research centers.

L'archive ouverte pluridisciplinaire **HAL**, est destinée au dépôt et à la diffusion de documents scientifiques de niveau recherche, publiés ou non, émanant des établissements d'enseignement et de recherche français ou étrangers, des laboratoires publics ou privés.



Comparison of ring currents evaluated consistently at Density Functional and Hartree-Fock levels

Journal:	<i>Molecular Physics</i>
Manuscript ID:	TMPH-2009-0319.R1
Manuscript Type:	Full Paper
Date Submitted by the Author:	23-Oct-2009
Complete List of Authors:	Havenith, Remco; Zernike Institute for Advanced Materials, University of Groningen, Theoretical Chemistry Meijer, Anthony; University of Sheffield, Department of Chemistry Irving, Benjamin; University of Sheffield, Department of Chemistry Fowler, Patrick; University of Sheffield, Department of Chemistry
Keywords:	Hartree-Fock, DFT, symmetry breaking, ring currents, aromaticity



1
2
3 **Comparison of ring currents evaluated consistently at Density Functional and**
4 **Hartree-Fock levels**
5
6
7

8 Remco W. A. Havenith^{a*}, Anthony J. H. M. Meijer^b, Benjamin J. Irving^b and Patrick
9 W. Fowler^b
10
11

12
13
14 ^a*Theoretical Chemistry, Zernike Institute for Advanced Materials,*
15 *University of Groningen, Nijenborgh 4, 9747 AG Groningen, The Netherlands.*

16 *E-mail: r.w.a.havenith@rug.nl*

17
18
19 ^b*Department of Chemistry, University of Sheffield, Sheffield S3 7HF, UK.*

20 *E-mail: A.Meijer@sheffield.ac.uk, P.W.Fowler@sheffield.ac.uk,*
21 *chp08bj@sheffield.ac.uk*
22
23
24
25
26
27
28
29

30 **Abstract**
31
32

33 Ring-current maps give an immediate visualisation of aromaticity on the magnetic
34 criterion - by which a cyclic system that supports diatropic (paratropic) current
35 induced by a perpendicular magnetic field is aromatic (anti-aromatic). Calculations of
36 maps with the ipsocentric choice of origin are made in the 6-31G** basis set at
37 Hartree Fock (HF) and Density Functional (DFT) levels (PW91 and B3LYP
38 functionals) on porphyrin, porphycene, orangarin, sapphyrin and hexabenzocoronene.
39 In these systems, DFT and HF approaches produce optimal geometries with different
40 point-group symmetries and/or different patterns of bond alternation. The ring-
41 current maps derived with all four combinations of methods indicate that the main
42 features of the current (global nature, direction, estimated strength) survive in systems
43 with symmetry-breaking, but that choice of geometry is more critical for the detail of
44 the current than is the electronic-structure method.
45
46
47
48
49
50
51
52
53
54
55
56
57
58
59
60

1 Introduction

Maps of the current density induced by an external magnetic field have been used to elucidate aromaticity of many molecules [1-11]. On the magnetic criterion, the ability to sustain a diatropic ring current is the defining characteristic of an aromatic system [12-17]. Visualisation of this current can give crucial details that are not obvious from integrated magnetic properties such as ^1H chemical shifts [14], Nucleus Independent Chemical Shifts (NICS) [18], exaltation of magnetisability [19] or magnetisability anisotropy [20], and calculation of the sense and strength of a global circulation gives a clear yes or no answer to the question of aromaticity on the magnetic criterion. Computation of ring currents within the ipsocentric [21] (CTOCD-*DZ*) approach [22-26] has the specific advantage that it provides uniquely defined orbital contributions [27], and it therefore allows the current to be rationalised in terms of virtual excitations from a given set of (canonical or localised) occupied orbitals to empty orbitals [28].

The ipsocentric method for the calculation of ring currents is economical in terms of basis set and has long been used at the Coupled Hartree-Fock (CHF) level of theory [22,24,26]. More recently it has been implemented within the framework of Density Functional Theory (DFT), where the contributions are defined for Kohn-Sham orbitals in a gauge-independent basis [29]. This approach has been used with a variety of functionals [30]. Other approaches to calculation of magnetic response properties at the DFT level mainly involve the use of Gauge-Including Atomic Orbitals [31-38].

For shieldings and other integrated properties, Hartree-Fock and DFT-based approaches can give results that differ significantly [30] but questions of aromaticity usually involve consideration of global patterns in the π currents, and hence currents in regions of molecular space that are not close to nuclei, and for such maps all initial indications [29,30] are that ipsocentric calculations at CHF and DFT levels are in excellent agreement, both at the qualitative level of assignment of a given system to aromatic, non-aromatic or anti-aromatic categories, and at the semi-quantitative level of the current strengths. The largest quantitative differences are found for systems dominated by paratropic response, i.e., anti-aromatics [29,30].

1
2
3
4
5
6
7
8
9
10
11
12
13
14
15
16
17
18
19
20
21
22
23
24
25
26
27
28
29
30
31
32
33
34
35
36
37
38
39
40
41
42
43
44
45
46
47
48
49
50
51
52
53
54
55
56
57
58
59
60

Where there is in fact a discernible difference between CHF and DFT current-density maps, it is natural to ascribe part of the discrepancy to variations between optimised geometries. In many cases, CHF currents themselves show only a weak dependence on the geometry used, whether HF-optimised, DFT-optimised or experimental [39,40], but sometimes HF and DFT geometries can differ drastically. In particular, it may happen that geometry optimisation at the Restricted Hartree-Fock (RHF) level leads to an equilibrium geometry with lower than expected symmetry, whereas DFT optimisation restores higher symmetry, leading to the suspicion that the RHF symmetry breaking is spurious. Examples of this particular version of the ‘symmetry dilemma’ have been encountered for a number of small molecules [41], and also for the larger systems to be discussed below. DFT and RHF geometries may also exhibit systematically divergent patterns of bond alternation [42], with DFT often tending to favour more ‘delocalised’ geometries [43]. All the molecules studied here have closed shells: the extent of symmetry-breaking in open-shell species such as the metallo-porphyrin π -cation radicals is the subject of a long-running debate [44].

An (untested) strategy for dealing with the dilemma, needed before DFT codes for current-density mapping became available, was to re-calculate the CHF current density or other magnetic properties at the DFT-optimised geometry [45], or constrain the RHF optimisation to the symmetry of the DFT structure. With the availability of a DFT ipsocentric code for the calculation of ring currents, the separate effects of geometry and electronic structure can now be studied. Here, we report maps of the induced current density evaluated consistently with two different functionals and compare them with maps obtained at both the CHF//RHF level, and at mixed CHF//DFT DFT//RHF levels (where // means ‘at the geometry of’) in order to help disentangle the influences of geometry, method and functional on induced current density.

2 Computational details

The molecules considered are (Scheme 1): porphyrin (1), porphycene (2), orangarin (3), sapphyrin (4) and hexabenzocoronene (5). They illustrate some of the possibilities for disagreement between HF and DFT approaches. The first two examples show broken symmetry. The porphyrin [46] framework would belong in

1
2
3
4
5
6
7
8
9
10
11
12
13
14
15
16
17
18
19
20
21
22
23
24
25
26
27
28
29
30
31
32
33
34
35
36
37
38
39
40
41
42
43
44
45
46
47
48
49
50
51
52
53
54
55
56
57
58
59
60

maximum symmetry to the D_{2h} point group [10], but when optimised at the RHF level under the D_{2h} constraints, it shows a large imaginary frequency ($\tilde{\nu} = 1718i \text{ cm}^{-1}$, RHF/6-31G**) for the mode representing distortion to C_{2v} ; with the B3LYP functional, maximum D_{2h} symmetry is retained, with the wavenumber for every vibrational mode exceeding 50 cm^{-1} (B3LYP/6-31G**). Similarly, porphycene [47,48] in C_{2h} symmetry is distortive towards planar C_s at the RHF level ($\tilde{\nu} = 1459i \text{ cm}^{-1}$, RHF/6-31G**), but has C_{2h} symmetry at the B3LYP/6-31G** DFT level. The expanded porphyrin, orangarin, and the polycyclic aromatic hydrocarbon, hexabenzocoronene, are examples of floppy molecules for which the symmetry of the global minimum is a delicate question. RHF calculations in high symmetry (C_{2v} and D_{6h} for **3** and **5**, respectively) show distortive modes with low imaginary frequencies ($38i$ and $20i \text{ cm}^{-1}$ for **3**, $23i$, $18i \text{ cm}^{-1}$ (doubly degenerate) for **5**) leading to non-planar structures (C_s and D_{3d} , respectively) that are almost iso-energetic with the higher-symmetry parent; B3LYP/6-31G** calculations, however, yield optimal geometries with the ideal higher symmetry in both cases. The remaining molecule on the list, sapphyrin, is again highly flexible, giving optimal geometries of C_{2v} symmetry at both RHF and DFT levels, but with low (real) frequencies for out-of-plane distortion (15 and 28 cm^{-1} RHF/6-31G**, 25 and 31 cm^{-1} B3LYP/6-31G**).

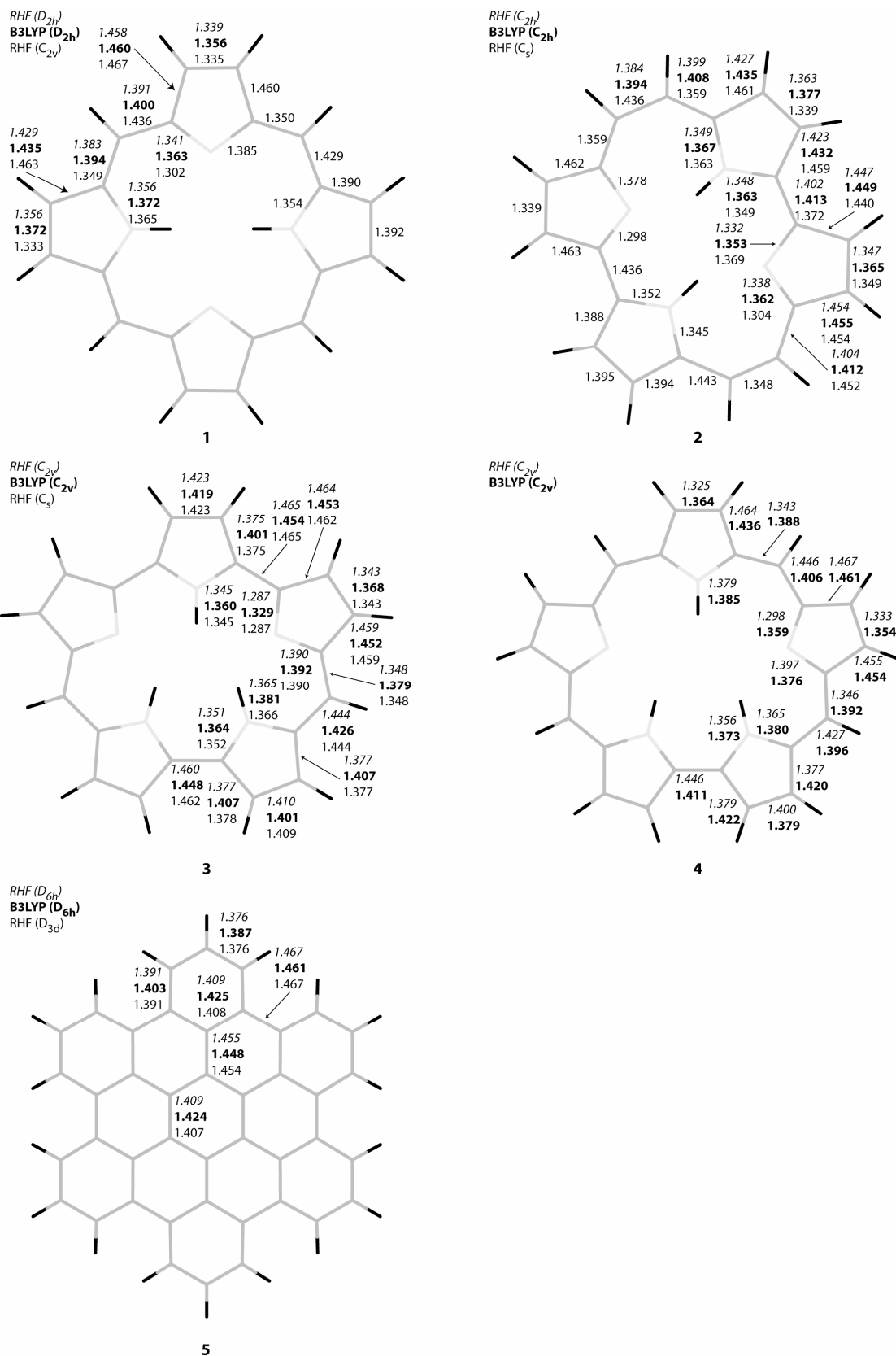
In detail, in the present work, geometries of **1-5** were re-optimised under constraints of high symmetry (**1**: D_{2h} ; **2**: C_{2h} ; **3**: C_{2v} ; **4**: C_{2v} ; **5**: D_{6h}) at the RHF/6-31G**, B3LYP/6-31G** and PW91/6-31G** levels of theory, using GAMESS-UK [49] and GAUSSIAN03 [50]. Evaluation of the Hessian showed that B3LYP/6-31G** and PW91/6-31G** optimised geometries were genuine minima, but the high-symmetry RHF/6-31G** optimised geometries for all but **4** were stationary points with at least one imaginary frequency. Relaxation and optimisation in lower symmetry resulted in RHF/6-31G** minima (**1**: C_{2v} ; **2**: C_s ; **3**: C_s ; **5**: D_{3d}). All geometries of **1**, **2**, **4** are planar; the low-symmetry forms of **3** and **5** are non-planar, with some rings bent slightly away from the median plane. Details of the computed bond lengths (RHF and B3LYP) are given in Scheme 1. For both **1** and **2**, the RHF geometries, constrained to D_{2h} and C_{2h} symmetry, respectively, and also the B3LYP optimal geometries, are very similar: on average, bond lengths are $\sim 0.01 \text{ \AA}$ longer at the B3LYP/6-31G** level of theory. Distortion to lower symmetry results in significant changes in bond lengths: the difference in bond length between a CC bond and its formerly symmetry related bond can be as large as 0.08 \AA . Also, a

1
2
3
4 considerable change of 0.04 Å in the CN bonds is found in the non-H bearing-pyrrole
5 rings. For **3** and **4**, the geometries calculated at the RHF and B3LYP levels differ: the
6 DFT bonds are not systematically longer in comparison with those obtained at the
7 RHF level, but alternate along the perimeter in such a way that the significant bond
8 length alternation found at the RHF level is damped at the B3LYP level. The
9 symmetry breaking at RHF/6-31G** for **3** is associated with an out-of-plane
10 movement of one of the pyrrole rings, but this has very little effect on the bond
11 lengths of the macrocycle. Also, for **5**, RHF/6-31G** predicts an out-of-plane
12 distortion of the outer benzenoid rings, which has little effect on the CC bond lengths
13 [51].

14
15
16
17
18
19
20
21 The current density induced by a perpendicular external magnetic field was
22 calculated at the CHF/6-31G** level for all RHF/6-31G** and B3LYP/6-31G**
23 geometries, at the B3LYP/6-31G** level for B3LYP and RHF optimal geometries,
24 and at the PW91/6-31G** level for PW91/6-31G** optimal geometry. The mapping
25 calculations followed the procedure described before [29] and used a combination of
26 GAMESS-UK and SYSMO [52] program packages. The ipsocentric method allows
27 decomposition of total induced current density into contributions from individual
28 molecular orbitals or subsets thereof [26]. In particular, this approach gives a well
29 defined separation into σ and π current densities. Typically, for conjugated systems,
30 the σ contributions are simply sums of localised bond circulations, and all the
31 interesting and characteristic features of these systems, such as ring currents, appear
32 in the π maps. Whereas the individual orbital contributions have a dependence on the
33 choice of molecular orbitals, the sums over σ and π manifolds are independent of
34 changes within the two sets, provided that the system is planar. In systems that depart
35 by only a small amount from planarity, approximate π maps can be constructed by
36 summing contributions of those orbitals of π ancestry [51]. In each map in the
37 present paper, the π current density is plotted in a plane $1a_0$ above the molecular plane
38 (or above the median plane) with standard plotting conventions [11]: contours denote
39 the modulus of the current density and arrows show its in-plane projection; anti-
40 clockwise circulations in the maps indicate diatropic, and clockwise paratropic,
41 current. The maximum value of the current per unit inducing field, j_{max} , taken over
42 the plotting plane, is given as a useful measure for comparison between different
43 versions of the map. For wider comparison, note that the yardstick for aromatic
44
45
46
47
48
49
50
51
52
53
54
55
56
57
58
59
60

1
2
3
4 currents, the π current in benzene, gives a value for j_{max} of 0.080 a.u. when calculated
5 in the standard plotting plane with the 6-31G** basis in both HF [53] and B3LYP
6 [29] approaches. Table 1 summarises the calculated energies, HOMO and LUMO
7 orbital energies and corresponding current strengths. As might be expected, the
8 HOMO-LUMO gaps are substantially larger at the RHF level than at DFT levels, with
9 unbound RHF LUMO energies. Symmetry breaking in the RHF calculation is
10 associated with widening of the HOMO-LUMO gap.
11
12
13
14
15
16
17
18
19
20
21
22
23
24
25
26
27
28
29
30
31
32
33
34
35
36
37
38
39
40
41
42
43
44
45
46
47
48
49
50
51
52
53
54
55
56
57
58
59
60

For Peer Review Only



Scheme 1

Table 1. Total energies (in au), HOMO and LUMO orbital energies (in eV), and maximum induced current densities (in au) for systems **1** to **5**, evaluated with different combinations of methods.

Molecule/Method	E_{tot}	E_{HOMO}	E_{LUMO}	j_{max}
(1) RHF//RHF (D_{2h})	-983.2809474	-5.94 (2a _u)	0.49 (4b _{1g})	0.172
(1) RHF//RHF (C_{2v})	-983.2871206	-6.41 (5a ₂)	0.87 (6a ₂)	0.095
(1) B3LYP//B3LYP (D_{2h})	-989.5777670	-5.16 (5b _{3u})	-2.25 (4b _{1g})	0.163
(1) RHF//B3LYP (D_{2h})	-983.2740146	-5.99 (2a _u)	0.37 (4b _{1g})	0.169
(1) B3LYP//RHF (C_{2v})	-989.5606716	-5.19 (8b ₁)	-2.13 (6a ₂)	0.138
(1) PW91//PW91 (D_{2h})	-989.2369599	-4.70 (5b _{3u})	-2.77 (4b _{1g})	0.159
(2) RHF//RHF (C_{2h})	-983.2724284	-6.16 (7a _u)	-0.29 (7b _g)	0.164
(2) RHF//RHF (C_s)	-983.2771868	-6.56 (13a'')	0.15 (14a'')	0.100
(2) B3LYP//B3LYP (C_{2h})	-989.5792685	-5.26 (7a _u)	-2.82 (7b _g)	0.150
(2) RHF//B3LYP (C_{2h})	-983.2637109	-6.19 (7a _u)	-0.39 (7b _g)	0.161
(2) B3LYP//RHF (C_s)	-989.5612540	-5.27 (13a'')	-2.69 (14a'')	0.133
(2) PW91//PW91 (C_{2h})	-989.2428382	-4.88 (7a _u)	-3.28 (7b _g)	0.145
(3) RHF//RHF (C_{2v})	-1114.0558408	-6.09 (7a ₂)	0.53 (9b ₁)	0.095
(3) RHF//RHF (C_s)	-1114.0559300	-6.10 (43a'')	0.53 (49a')	0.102
(3) B3LYP//B3LYP (C_{2v})	-1121.1355006	-4.50 (7a ₂)	-2.87 (9b ₁)	0.224
(3) RHF//B3LYP (C_{2v})	-1114.0413415	-5.82 (7a ₂)	0.14 (9b ₁)	0.115
(3) B3LYP//RHF (C_s)	-1121.1223497	-4.64 (43a'')	-2.64 (49a')	0.145
(3) PW91//PW91 (C_{2v})	-1120.7592614	-4.07 (7a ₂)	-3.44 (9b ₁)	0.315
(4) RHF//RHF (C_{2v})	-1190.9412672	-6.14 (7a ₂)	0.69 (8a ₂)	0.086
(4) B3LYP//B3LYP (C_{2v})	-1198.5514649	-4.78 (9b ₁)	-2.40 (8a ₂)	0.189
(4) RHF//B3LYP (C_{2v})	-1190.9176528	-5.71 (7a ₂)	0.14 (8a ₂)	0.157
(4) B3LYP//RHF (C_{2v})	-1198.5308575	-4.96 (9b ₁)	-2.28 (8a ₂)	0.130
(4) PW91//PW91 (C_{2v})	-1198.1428152	-4.39 (9b ₁)	-2.86 (8a ₂)	0.187
(5) RHF//RHF (D_{3d})	-1601.2049304	-6.71 (23e _g)	1.62 (22e _u)	0.112
(5) B3LYP//B3LYP (D_{6h})	-1611.5492384	-5.25 (4e _{1g})	-1.66 (4e _{2u})	0.103
(5) PW91//PW91 (D_{6h})	-1610.9681763	-4.80 (4e _{1g})	-2.32 (4e _{2u})	0.102

3 Current-density maps

Figures 1 to 5 show the maps of π current density calculated for molecules **1** to **5**.

Porphyrim (1): The three consistently evaluated maps (top row, Figure 1) all show a global diatropic ring current, and hence predict aromaticity for this macrocycle. The circulation is weakest in the symmetry-broken CHF//RHF map (top right in the figure), but even here is still ~20% stronger than the 'standard' benzene π current, as judged by values of j_{max} (Table 1). All maps computed for geometries of D_{2h} symmetry are closely similar in appearance, all indicating a macrocyclic current that is twice as strong as the ring current in benzene, bifurcated in the two H-bearing pyrrole rings, and avoiding the CC bonds of the other five-membered rings. Apart from the relative intensity of the currents, the main difference in detail between the maps evaluated for C_{2v} and D_{2h} geometries is that the symmetry breaking renders the H-bearing pyrrole rings inequivalent, leading to the current taking the inside path in one case and the outside path in the other. This asymmetry is reduced but not eliminated in the map calculated for this RHF geometry at the DFT level. In spite of the differences between the RHF D_{2h} -constrained and DFT fully optimal D_{2h} geometries (Scheme 1), the chemical interpretation of the maps is identical. This provides a *post hoc* justification for use of symmetry constraints [10,54,55] or taking DFT geometries in CHF calculations of current [48,56].

The broad agreement between RHF and DFT maps calculated at similar geometries is readily understood in terms of the orbital model [10,26] of induced current. Ipsocentrally calculated currents can be accounted for in terms of virtual excitations from occupied to empty frontier orbitals obeying selection rules that are based on nodal character of the orbitals involved. Orbital energy differences modify the strength of the contribution, but in the absence of major topological changes to the orbitals, the origin of the major contributions to current remains unaffected. Detailed consideration of orbital contributions [29] suggests that the orbital picture survives the change from RHF MOs to KS orbitals, despite minor reordering of energies. In this respect, KS orbitals, though fictitious, are useful [57]. This was checked in the present case by explicit computation and mapping of orbital contributions. The current density in porphyrin is dominated by the four electrons in the HOMO and

1
2
3 HOMO-1 and their excitations to the LUMO and LUMO+1 in both RHF [10] and
4 DFT models, despite the fact that the RHF HOMO and HOMO-1 swap over at the
5 B3LYP level.
6
7

8
9 *Porphycene (2)*: The maps for porphycene display the same trends as those for
10 porphyrin: relative weakness of the current in the symmetry-broken CHF//RHF map
11 (here C_s), uniformity of all maps in the higher symmetry (here C_{2h}) and differences in
12 detail of the bifurcation pattern, which is partly recovered at the DFT//RHF level.
13
14 Again, chemical interpretation in terms of aromaticity is unaffected by the precise
15 details of the calculation, all maps showing a global diatropic ring current, of about
16 twice the strength of the benzene current in high symmetry cases.
17
18

19
20
21 *Orangarin (3)*: This system differs from (1) and (2) in that the predicted global
22 current is paratropic and hence the system is anti-aromatic. All six maps in Figure 3
23 show a current that has this sense of circulation, but now the predicted intensity is
24 strongly dependent on calculation type, functional and geometry. The three
25 consistently calculated maps (top row, Figure 3) show a variation of a factor of three
26 in j_{max} , both DFT maps exhibiting much larger currents than predicted by the CHF
27 calculation, and with the strength of current following the trend in the HOMO-LUMO
28 gap. These large differences outweigh the minor effects of geometry and symmetry
29 change shown by the remaining maps.
30
31
32
33
34
35
36

37 The distinction between (3) and the relatively insensitive diatropic systems (1) and
38 (2) is easily rationalised on the orbital model of induced currents [21,26]. In
39 cylindrical symmetry, diatropic currents arise from virtual transitions between orbitals
40 that differ by one unit in angular momentum (one in the number of angular nodes) and
41 are typically separated by a substantial energy gap. In contrast, paratropic currents
42 arise from virtual excitations between occupied and unoccupied members of a pair
43 with the same angular momentum, which are typically separated by a small splitting
44 (arising for example from the Jahn-Teller effect). As such, paratropic currents are
45 expected to be more sensitive to the size of the HOMO-LUMO gap, and hence to
46 electron correlation. Sensitivity to calculation type (HF or DFT) and to functional
47 have been noted in mapping of the paratropic current in (planarised) cyclooctatetraene
48 [29,30], and has the same rationale as in the present case. In spite of the difficulty of
49 obtaining a precise value for the current, which is reflected in the sensitivity of NMR
50 parameters to the method of calculation [30], the qualitative interpretation remains
51 clear: free-base orangarin is an anti-aromatic compound.
52
53
54
55
56
57
58
59
60

1
2
3
4
5
6
7
8
9
10
11
12
13
14
15
16
17
18
19
20
21
22
23
24
25
26
27
28
29
30
31
32
33
34
35
36
37
38
39
40
41
42
43
44
45
46
47
48
49
50
51
52
53
54
55
56
57
58
59
60

Sapphyrin (**4**): Here, there is no difference in symmetry between HF and DFT optimal geometries. However, the maps show strong differences between CHF//RHF and other levels. When the HF level is consistently applied, the resulting map has only a weak diatropic perimetric circulation (1.1 times the strength of the benzene π current). All the other maps show significantly stronger diatropic macrocyclic circulations with similar strengths for both functionals (B3LYP: 2.4 times the standard benzene value, PW91 2.3 times, Table 1). The maps calculated consistently at the DFT levels show a bifurcation in all five pyrrole rings. This detail is not reproduced at the CHF//RHF level where two of the rings show evidence of small, local diatropic ring currents within the pyrrole subunits. The major difference between the CHF//RHF map and all others is presumably ultimately attributable to the strong variation in the degree of bond alternation (Scheme 1) between RHF and DFT optimal geometries, although it apparently requires the combination of localised electronic structure with a localised underlying geometry to reduce the ring current of the macrocycle. Nevertheless, at the 'yes/no' level of chemical interpretation, all maps indicate aromaticity for sapphyrin (**4**), and all but one agree on the main pathway for the current.

Hexabenzocoronene (**5**): The three consistently computed maps for this molecule (Figure 5) are essentially identical, indicating that the small geometrical changes accompanying symmetry breaking at the RHF level are ineffective in changing the current map. All three maps show the superposition of local Clar-sextet diatropic ring currents and overall diatropic perimeter current that is characteristic of totally-resonant-sextet benzenoids [58]. The qualitative chemical interpretation of the magnetic response of this molecule remains unchanged from that given in Ref. [51]. As has been found for clamped aromatic and anti-aromatic systems, current can survive a significant degree of bond alternation, provided that there is no essential alteration in the nodal structure of the magnetically active frontier orbitals [3,59]. Small out-of-plane distortions in **5** evidently do not alter this structure, which is common to both HF and KS frontier orbitals.

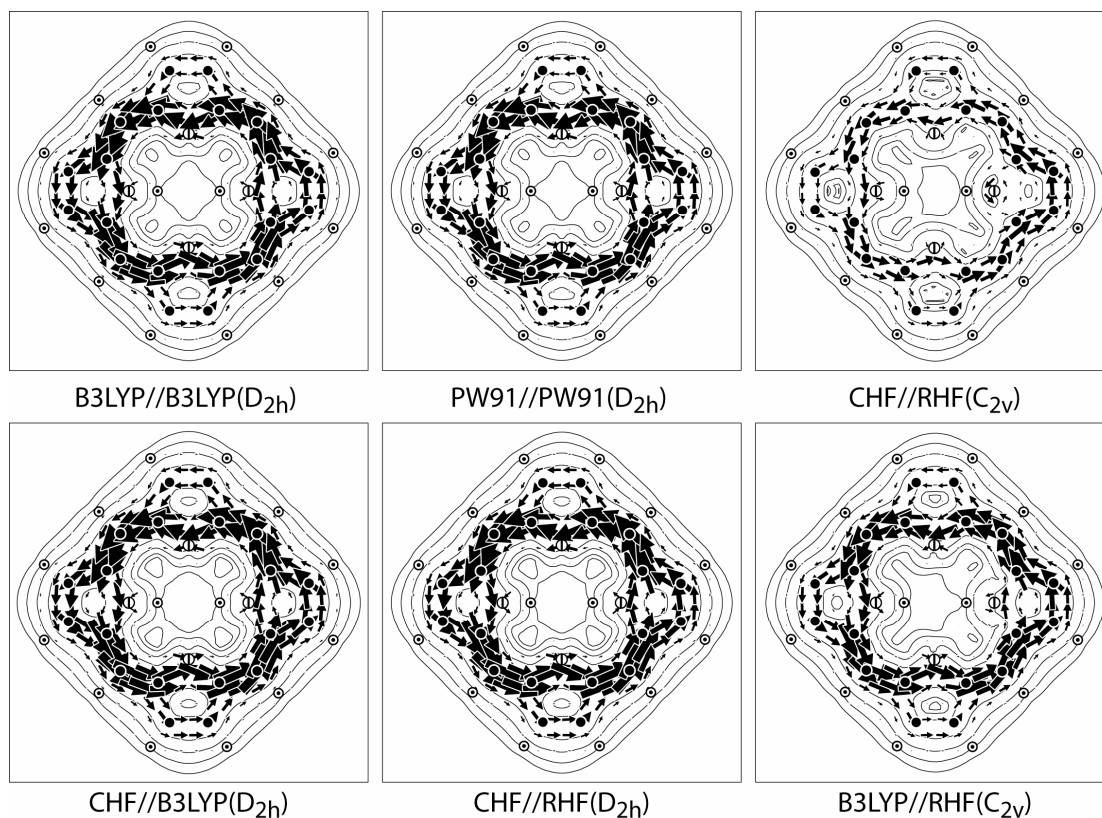


Figure 1. Maps of the π -current density calculated for porphyrin (**1**) at different levels of theory, all in the 6-31G** basis set. Plotting conventions are described in the text.

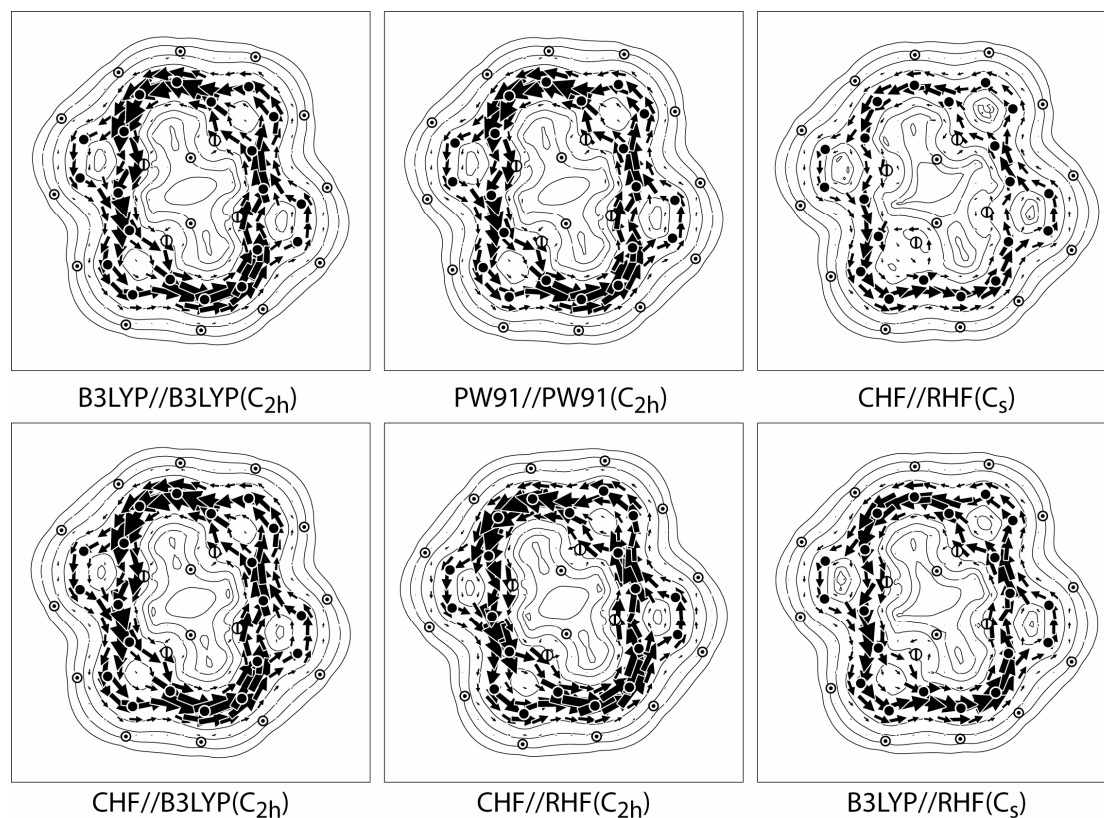


Figure 2. Maps of the π -current density calculated for porphycene (2) at different levels of theory, all in the 6-31G** basis set. Plotting conventions are described in the text.

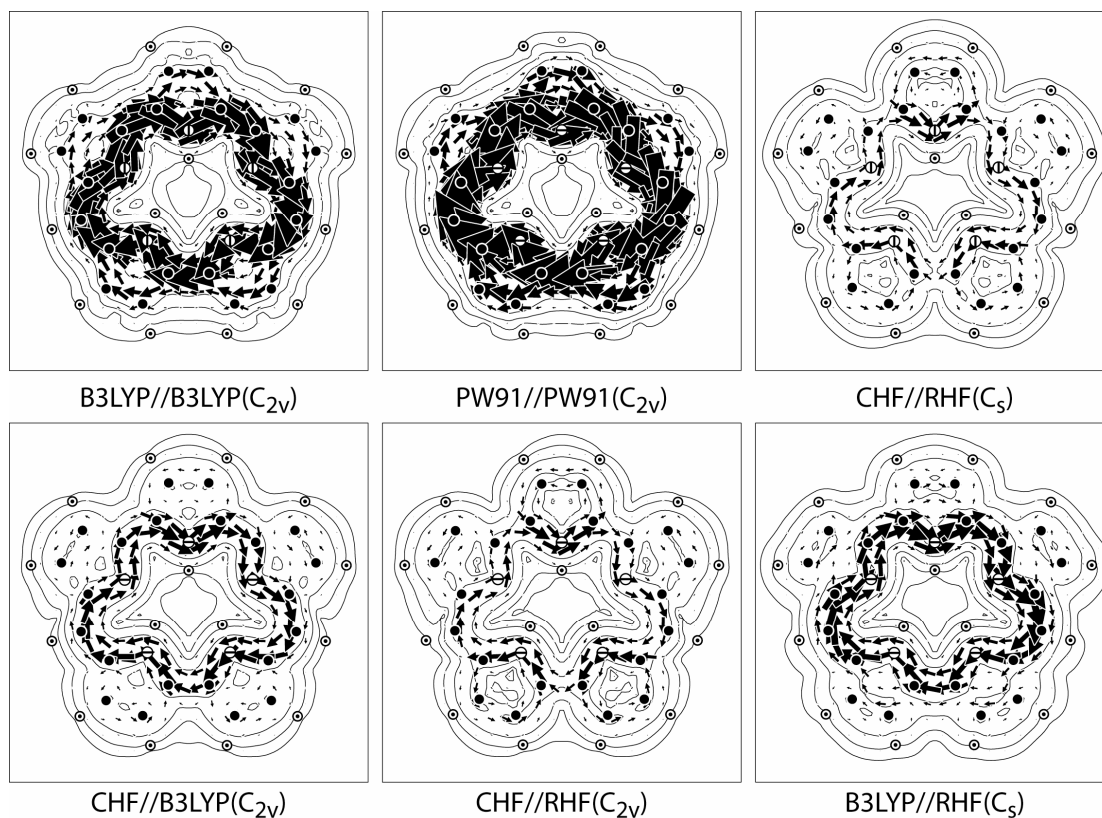


Figure 3. Maps of the π -current density calculated for orangarin (**3**) at different levels of theory, all in the 6-31G** basis set. Plotting conventions are described in the text.

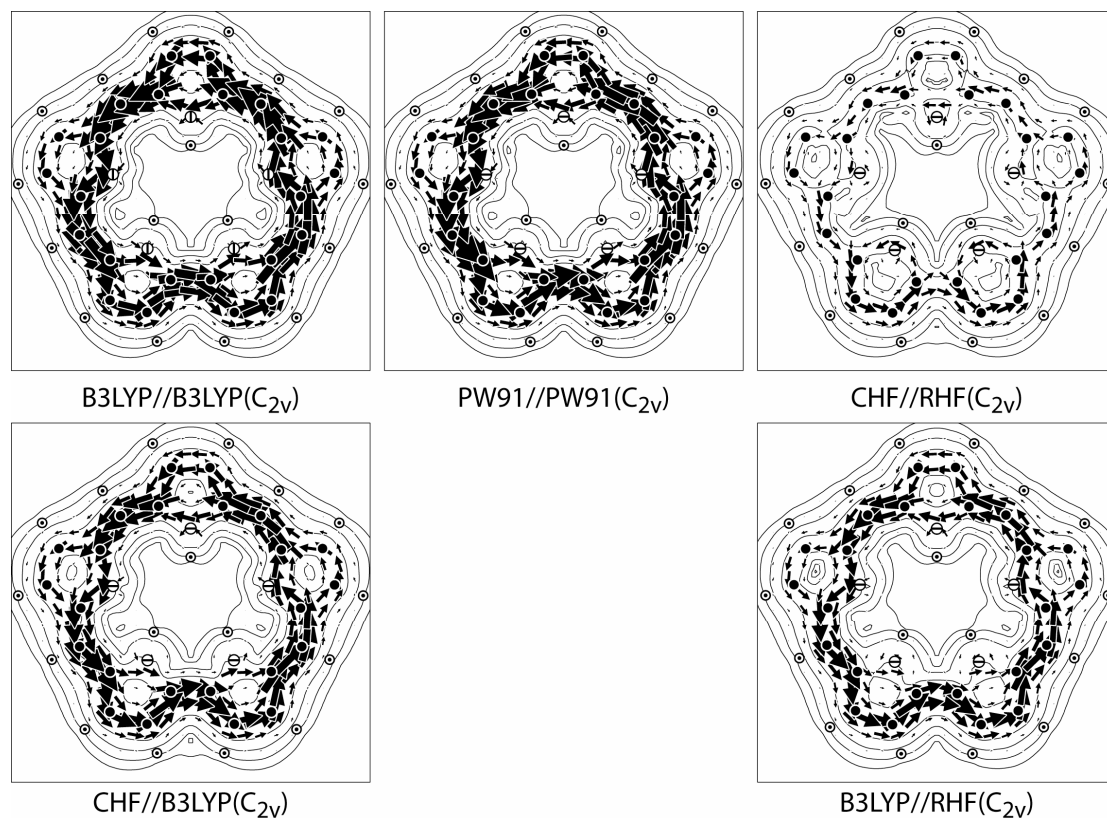


Figure 4. Maps of the π -current density calculated for saphyrin (4) at different levels of theory, all in the 6-31G** basis set. Plotting conventions are described in the text.

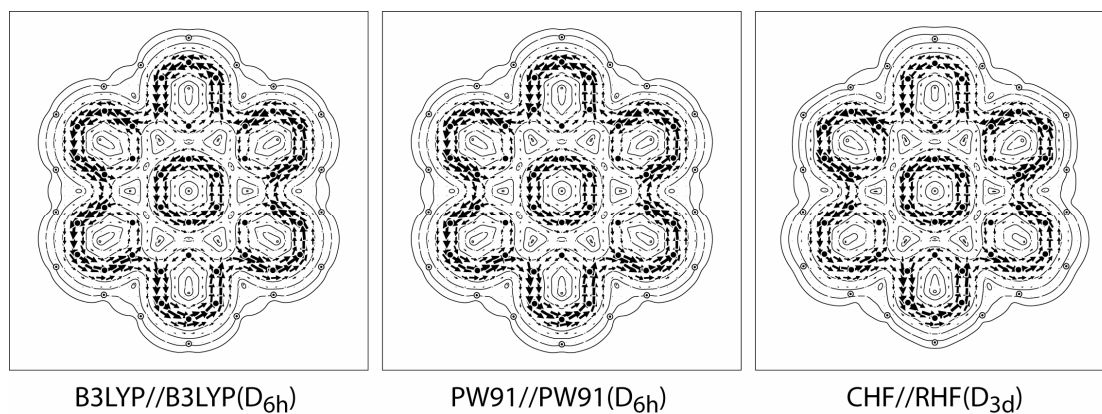


Figure 5. Maps of the π -current density calculated for hexabenzocoronene (5) at different levels of theory, all in the 6-31G** basis set. Plotting conventions are described in the text.

4 Conclusions

A short survey has been made of some molecules where correlation effects as represented by DFT functionals have a significant effect on predicted molecular symmetry and patterns of bond lengths. At the gross level of prediction of aromatic/anti-aromatic character through the qualitative characteristics of the induced current density, it appears that HF and DFT methods in any combination give the same verdict, but at the semi-quantitative level of the current strength, consistent results are obtained with both methods only where the DFT geometrically delocalised structure is employed. The recommendation is to use this structure.

The qualitative similarity of all methods, regardless of geometric detail, follows from the general ipsocentric explanation of induced current in terms in nodal character of the frontier orbitals. Conversely, the sensitivity of the systems with dominant paratropic currents also follows from this global explanation as a consequence of sensitivity to HOMO-LUMO gap of the important frontier-orbital contribution.

Detailed comparison of the properties that arise from integration of the current density (such as magnetisability, nuclear shieldings and chemical shifts) has not been attempted here. Experience with variants on the ipsocentric method [25] indicates that for these properties, which depend on the total current density and on features close to nuclei, the PZ2 choice of origin is numerically superior to the pure ipsocentric (DZ) strategy, even if both methods give essentially perfect agreement for the π current-density maps from which assignments of aromaticity are determined [60]. Experience with calculation of magnetic properties with DFT methods [30,34] shows that good results for chemical shifts can be obtained with appropriately chosen functionals. The present study has added another strand to the discussion, in indicating that an appropriate geometry is important too, especially in symmetry-broken cases.

Acknowledgment

PWF thanks the Royal Society/Wolfson Scheme for financial support through a Research Merit Award. BJI thanks EPSRC for a DTA studentship.

References

- [1] U. Fleischer, W. Kutzelnigg, P. Lazzeretti, and V. Muhlenkamp, *J. Am. Chem. Soc.* **116**, 5298 (1994).
- [2] A. Ligabue, U. Pincelli, P. Lazzeretti, and R. Zanasi, *J. Am. Chem. Soc.* **121**, 5513 (1999).
- [3] P. W. Fowler, R. W. A. Havenith, L. W. Jenneskens, A. Soncini, and E. Steiner, *Chem. Commun.*, 2386 (2001).
- [4] P. W. Fowler, R. W. A. Havenith, and E. Steiner, *Chem. Phys. Lett.* **359**, 530 (2002).
- [5] S. Pelloni, and P. Lazzeretti, *Theor. Chem. Acc.* **117**, 903 (2007).
- [6] J. Juselius, and D. Sundholm, *Phys. Chem. Chem. Phys.* **10**, 6630 (2008).
- [7] G. Monaco, and R. Zanasi, *J. Phys. Chem. A* **112**, 8136 (2008).
- [8] I. G. Cuesta, A. S. De Meras, S. Pelloni, and P. Lazzeretti, *J. Comp. Chem.* **30**, 551 (2009).
- [9] P. W. Fowler, N. Mizoguchi, D. E. Bean, and R. W. A. Havenith, *Chem. Eur. J.* **15**, 6964 (2009).
- [10] E. Steiner, and P. W. Fowler, *Chem. Phys. Chem.* **3**, 114 (2002).
- [11] E. Steiner, P. W. Fowler, and L. W. Jenneskens, *Angew. Chem. Int. Ed.* **40**, 362 (2001).
- [12] L. Pauling, *J. Chem. Phys.* **4**, 673 (1936).
- [13] F. London, *J. Phys. Radium* **8**, 397 (1937).
- [14] J. Pople, *J. Chem. Phys.* **24**, 1111 (1956).
- [15] J. A. Elvidge, and L. M. Jackman, *J. Chem. Soc.*, 859 (1961).
- [16] P. von R. Schleyer, and H. Jiao, *Pure Appl. Chem.* **68**, 209 (1996).
- [17] J. A. N. F. Gomes, and R. B. Mallion, *Chem. Rev.* **101**, 1349 (2001).
- [18] P. von R. Schleyer, C. Maerker, A. Dransfeld, H. Jiao, and N. J. R. van Eikema Hommes, *J. Am. Chem. Soc.* **118**, 6317 (1996).
- [19] H. J. Dauben, J. D. Wilson, and J. L. Laity, *J. Am. Chem. Soc.* **91**, 1991 (1969).
- [20] W. H. Flygare, *Chem. Rev.* **74**, 653 (1974).
- [21] E. Steiner, and P. W. Fowler, *Chem. Commun.*, 2220 (2001).
- [22] T. Keith, and R. F. W. Bader, *Chem. Phys. Lett.* **210**, 223 (1993).

- 1
2
3 [23] S. Coriani, P. Lazzeretti, M. Malagoli, and R. Zanasi, *Theor. Chim. Acta* **89**,
4 181 (1994).
5
6 [24] P. Lazzeretti, M. Malagoli, and R. Zanasi, *Chem. Phys. Lett.* **220**, 299 (1994).
7
8 [25] R. Zanasi, *J. Chem. Phys.* **105**, 1460 (1996).
9
10 [26] E. Steiner, and P. W. Fowler, *J. Phys. Chem. A* **105**, 9553 (2001).
11
12 [27] E. Steiner, and P. W. Fowler, *Phys. Chem. Chem. Phys.* **6**, 261 (2004).
13
14 [28] E. Steiner, P. W. Fowler, and R. W. A. Havenith, *J. Phys. Chem. A* **106**, 7048
15 (2002).
16
17 [29] R. W. A. Havenith, and P. W. Fowler, *Chem. Phys. Lett.* **449**, 347 (2007).
18
19 [30] A. Soncini, A. M. Teale, T. Helgaker, F. De Proft, and D. J. Tozer, *J. Chem.*
20 *Phys.* **129**, 074101 (2008).
21
22 [31] V. G. Malkin, O. L. Malkina, M. E. Casida, and D. R. Salahub, *J. Am. Chem.*
23 *Soc.* **116**, 5898 (1994).
24
25 [32] T. Helgaker, P. J. Wilson, R. D. Amos, and N. C. Handy, *J. Chem. Phys.* **113**,
26 2983 (2000).
27
28 [33] F. De Proft, P. von R. Schleyer, J. H. van Lenthe, F. Stahl, and P. Geerlings,
29 *Chem. Eur. J.* **8**, 3402 (2002).
30
31 [34] M. J. Allen, T. W. Keal, and D. J. Tozer, *Chem. Phys. Lett.* **380**, 70 (2003).
32
33 [35] K. Najafian, P. von R. Schleyer, and T. T. Tidwell, *Org. Biomol. Chem.* **1**,
34 3410 (2003).
35
36 [36] T. Heine, C. Corminboeuf, G. Grossmann, and U. Haeberlen, *Angew. Chem.*
37 *Int. Ed.* **45**, 7292 (2006).
38
39 [37] A. Ligabue, S. P. A. Sauer, and P. Lazzeretti, *J. Chem. Phys.* **126**, 154111
40 (2007).
41
42 [38] S. Taubert, D. Sundholm, J. Juselius, W. Klopper, and H. Fliegl, *J. Phys.*
43 *Chem. A* **112**, 13584 (2008).
44
45 [39] M. K. Cyranski, R. W. A. Havenith, M. A. Dobrowolski, B. R. Gray, T. M.
46 Krygowski, P. W. Fowler, and L. W. Jenneskens, *Chem. Eur. J.* **13**, 2201
47 (2007).
48
49 [40] P. W. Fowler, M. Lillington, and L. P. Olson, *Pure Appl. Chem.* **79**, 969
50 (2007).
51
52 [41] C. D. Sherrill, M. S. Lee, and M. Head-Gordon, *Chem. Phys. Lett.* **302**, 425
53 (1999).
54
55
56
57
58
59
60

- 1
2
3
4 [42] W. Koch, and M. C. Holthausen: A Chemist's Guide to Density Functional
5 Theory, Wiley-VCH, New York, 2001.
6
7 [43] A. Soncini, P. W. Fowler, and L. W. Jenneskens, *Phys. Chem. Chem. Phys.* **6**,
8 277 (2004).
9
10 [44] T. Vangberg, R. Lie, and A. Ghosh, *J. Am. Chem. Soc.* **124**, 8122 (2002).
11
12 [45] J. Juselius, and D. Sundholm, *Phys. Chem. Chem. Phys.* **2**, 2145 (2000).
13
14 [46] J. Baker, P. M. Kozłowski, A. A. Jarzecki, and P. Pulay, *Theor. Chem. Acc.*
15 **97**, 59 (1997).
16
17 [47] P. M. Kozłowski, M. Z. Zgierski, and J. Baker, *J. Chem. Phys.* **109**, 5905
18 (1998).
19
20 [48] E. Steiner, and P. W. Fowler, *Org. Biomol. Chem.* **1**, 1785 (2003).
21
22 [49] M. F. Guest, I. J. Bush, H. J. J. van Dam, P. Sherwood, J. M. H. Thomas, J. H.
23 van Lenthe, R. W. A. Havenith, and J. Kendrick, *Mol. Phys.* **103**, 719 (2005).
24
25 [50] M. J. Frisch, G. W. Trucks, H. B. Schlegel, G. E. Scuseria, M. A. Robb, J. R.
26 Cheeseman, J. J. A. Montgomery, T. Vreven, K. N. Kudin, J. C. Burant, J. M.
27 Millam, S. S. Iyengar, J. Tomasi, V. Barone, B. Mennucci, M. Cossi, G.
28 Scalmani, N. Rega, G. A. Petersson, H. Nakatsuji, M. Hada, M. Ehara, K.
29 Toyota, R. Fukuda, J. Hasegawa, M. Ishida, T. Nakajima, Y. Honda, O. Kitao,
30 H. Nakai, M. Klene, X. Li, J. E. Knox, H. P. Hratchian, J. B. Cross, V.
31 Bakken, C. Adamo, J. Jaramillo, R. Gomperts, R. E. Stratmann, O. Yazyev, A.
32 J. Austin, R. Cammi, C. Pomelli, J. W. Ochterski, P. Y. Ayala, K. Morokuma,
33 G. A. Voth, P. Salvador, J. J. Dannenberg, V. G. Zakrzewski, S. Dapprich, A.
34 D. Daniels, M. C. Strain, O. Farkas, D. K. Malick, A. D. Rabuck, K.
35 Raghavachari, J. B. Foresman, J. V. Ortiz, Q. Cui, A. G. Baboul, S. Clifford, J.
36 Cioslowski, B. B. Stefanov, G. Liu, A. Liashenko, P. Piskorz, I. Komaromi, R.
37 L. Martin, D. J. Fox, T. Keith, M. A. Al-Laham, C. Y. Peng, A. Nanayakkara,
38 M. Challacombe, P. M. W. Gill, B. Johnson, W. Chen, M. W. Wong, C.
39 Gonzalez, and J. A. Pople, Gaussian 03, Revision B.01, Gaussian, Inc.,
40 Pittsburgh PA
41
42 [51] A. Soncini, E. Steiner, P. W. Fowler, R. W. A. Havenith, and L. W.
43 Jenneskens, *Chem. Eur. J.* **9**, 2974 (2003).
44
45 [52] P. Lazzeretti, and R. Zanasi, SYSMO package (University of Modena), 1980.
46 Additional routines by P. W. Fowler, E. Steiner, R. W. A. Havenith, A.
47 Soncini.
48
49
50
51
52
53
54
55
56
57
58
59
60

- 1
2
3 [53] E. Steiner, and P. W. Fowler, *Int. J. Quantum Chem.* **60**, 609 (1996).
4
5 [54] E. Steiner, and P. W. Fowler, in B. Grimm, R. Porra, W. Rüdiger, H. Scheer
6 (Eds.), *Chlorophylls and Bacteriochlorophylls: Biochemistry, Biophysics,*
7 *Functions and Applications.* Springer, Dordrecht, The Netherlands, ISBN
8 1402045158, 2006.
9
10 [55] E. Steiner, A. Soncini, and P. W. Fowler, *Org. Biomol. Chem.* **3**, 4053 (2005).
11
12 [56] E. Steiner, and P. W. Fowler, *Org. Biomol. Chem.* **4**, 2473 (2006).
13
14 [57] S. Hamel, P. Duffy, M. E. Casida, and D. R. Salahub, *J. Elec. Spec. Rel. Phen.*
15 **123**, 345 (2002).
16
17 [58] E. Steiner, P. W. Fowler, A. Soncini, and L. W. Jenneskens, *Faraday*
18 *Discussions* **135**, 309 (2007).
19
20 [59] P. W. Fowler, R. W. A. Havenith, L. W. Jenneskens, A. Soncini, and E.
21 Steiner, *Angew. Chem. Int. Ed. Engl.* **41**, 1558 (2002).
22
23 [60] A. Soncini, and P. W. Fowler, *Chem. Phys. Lett.* **396**, 174 (2004).
24
25
26
27
28
29
30
31
32
33
34
35
36
37
38
39
40
41
42
43
44
45
46
47
48
49
50
51
52
53
54
55
56
57
58
59
60